Animal Nutrition 16 (2024) 409–421

Contents lists available at ScienceDirect

Animal Nutrition

journal homepage: http://www.keaipublishing.com/en/journals/aninu/

Original Research Article

Retinoic acid alleviates rotavirus-induced intestinal damage by regulating redox homeostasis and autophagic flux in piglets

Xin Lai [a, 1], Aimin Wu [a, b, 1], Bing Yu [a, b], Hui Yan [a, b], Junqiu Luo [a, b], Ping Zheng [a, b], Jie Yu [a, b], Daiwen Chen [a, b, *]

[a] Institute of Animal Nutrition, Sichuan Agricultural University, Chengdu, China
[b] Key Laboratory for Animal Disease-resistance Nutrition of China Ministry of Education, Sichuan Agricultural University, Chengdu, China

ARTICLE INFO

Article history:
Received 8 April 2023
Received in revised form
11 December 2023
Accepted 28 December 2023
Available online 20 January 2024

Keywords:
Rotavirus
Piglet
Retinoic acid
Intestinal barrier
Redox hemostasis
Autophagic flux

ABSTRACT

Rotaviruses (RV) are a major cause of severe gastroenteritis, particularly in neonatal piglets. Despite the availability of effective vaccines, the development of antiviral therapies for RV remains an ongoing challenge. Retinoic acid (RA), a metabolite of vitamin A, has been shown to have anti-oxidative and antiviral properties. However, the mechanism by which RA exerts its intestinal-protective and antiviral effects on RV infection is not fully understood. The study investigates the effects of RA supplementation in Duroc × Landrace × Yorkshire (DLY) piglets challenged with RV. Thirty-six DLY piglets were assigned into six treatments, including a control group, RA treatment group with two concentration gradients (5 and 15 mg/d), RV treatment group, and RV treatment group with the addition of different concentration gradients of RA (5 and 15 mg/d). Our study revealed that RV infection led to extensive intestinal architecture damage, which was mitigated by RA treatment at lower concentrations by increasing the villus height and villus height/crypt depth ratio ($P < 0.05$), enhancing intestinal stem cell signaling and promoting intestinal barrier functions. In addition, 15 mg/d RA supplementation significantly increased NRF2 and HO-1 protein expression ($P < 0.05$) and GSH content ($P < 0.05$), indicating that RA supplementation can enhance anti-oxidative signaling and redox homeostasis after RV challenge. Additionally, the research demonstrated that RA exerts a dual impact on the regulation of autophagy, both stimulating the initiation of autophagy and hindering the flow of autophagic flux. Through the modulation of autophagic flux, RA influence the progression of RV infection. These findings provide new insights into the regulation of redox hemostasis and autophagy by RA and its potential therapeutic application in RV infection.

1. Introduction

Rotavirus (RV) is a major cause of gastroenteritis in young children worldwide. It has been estimated that RV is responsible for approximately 215,000 deaths annually, with most of the deaths occurring in low-income countries (Minton, 2022). In the pig industry, RV is also an emerging pathogen that is currently recognized as the major cause of gastroenteritis in neonatal piglets, resulting in substantial economic losses (Guo et al., 2022). Previous studies have demonstrated that RV infection induces apoptosis in enterocytes, leading to the loss of epithelial integrity and barrier function (Sen et al., 2020). In addition to apoptosis, RV infection also leads to villus atrophy, crypt hyperplasia, malabsorption, and a decrease in the levels of intestinal brush border enzymes, leading to severe diarrhea and dehydration (Stanifer and Boulant, 2020).

Autophagy is a natural and conserved process that involves the degradation of unnecessary or dysfunctional components of a cell through a lysosome-dependent mechanism (Qian et al., 2017). It has been found to be a critical regulator of host cells' antiviral signaling. The relationship between autophagy and virus infection

* Corresponding author.
E-mail address: dwchen@sicau.edu.cn (D. Chen).
[1] These authors contributed equally to this work.
Peer review under responsibility of Chinese Association of Animal Science and Veterinary Medicine.

Production and Hosting by Elsevier on behalf of KeAi

https://doi.org/10.1016/j.aninu.2023.12.007

is not one-way, and it is closely related to the stage of viral infection. The effect of autophagy regulation on the virus in infected organisms is complex and can present both similarities and distinctions in various viruses (Moroso et al., 2022; Xiao and Cai, 2020). The articles on RV infection and autophagy also have contradictory points. One study showed that RV infection induces lipidation of the autophagy marker protein, microtubule-associated protein light chain 3 (LC3), and that membranes containing LC3 and the RV glycoprotein NSP4 traffic to viroplasms, suggesting that NSP4 must exit the endoplasmic reticulum (ER) (Crawford et al., 2019). Crawford conducted a study and discovered that RV infection suppresses autophagy maturation (Crawford et al., 2012). In addition, a study showed that vitamin D_3 supplementation can alleviate RV infection in pigs and cells by activating autophagy (Tian et al., 2016). A different investigation revealed the phosphoinositide 3-kinase (PI3K)-protein kinase B (Akt)-mammalian target of rapamycin (mTOR) axis sustains RV infection via the eukaryotic translation initiation factor 4E-binding protein 1 (4E-BP1) mediated autophagy pathway and represents an antiviral target (Yin et al., 2018). Overall, further research is needed to fully understand the mechanisms by which RV infection affects autophagy.

Besides autophagy, RV infection can lead to changes in oxidative status in host cells. Studies have shown that RV can cause an imbalance between production of oxidants and antioxidant defenses, resulting in oxidative stress (Guerrero and Acosta, 2016). This is likely due to the interaction between virion proteins and various cell surface molecules during RV entry into the host cell (Guerrero and Acosta, 2016). One study found that RV infection caused a decrease in the ratio between reduced glutathione (GSH) and oxidized GSH (GSSG), which was also observed when purified NSP4 was added to Caco-2 cells (Buccigrossi et al., 2014). In addition, findings from a study unveiled that the modulation of the nuclear factor erythroid 2-related factor 2 (NRF2)-based host cellular redox defense system declines sharply in response to RV infection in vitro (Patra et al., 2020). These studies suggest that RV infection can cause an imbalance in oxidative status, leading to oxidative stress and potential damage to biological systems.

Retinoic acid (RA) is a metabolite of vitamin A that has diverse biological activities and regulates several cellular functions (Szymański et al., 2020). Recent studies have investigated the role of RA in autophagy and have shown that it can promote autophagosome maturation and induce autophagy in Toll-like receptor (TLR)-activated B cells (Rajawat et al., 2011; Wang et al., 2021). Furthermore, all-trans RA has been demonstrated to promote autophagy and restore gene expression associated with autophagy in an acute promyelocytic leukemia model (Cao et al., 2018). RA-induced autophagy is mediated through different pathways that may be independent of the classic nuclear retinoid receptors (Rajawat et al., 2010). In summary, RA has been shown to have a role in regulating autophagy in different cell types through different pathways. The potential of RA to alleviate RV infection by regulating autophagy requires further investigation.

Previous studies also have demonstrated that RA possesses certain antioxidant properties. A study has investigated all-trans RA prevented oxidative stress-induced loss of renal tight junction proteins in a type-1 diabetic model (Molina-Jijón et al., 2015). However, research on RA in piglets is still relatively limited. Findings from a study indicate that RA suppresses the retinoic acid-inducible gene I (RIG-I)-like receptors (RLRs)/nuclear factor kappa B (NF-κB) signaling pathway, leading to the reduction of inflammation induced by transmissible gastroenteritis virus (TGEV) in IPEC-J2 cells (Pu et al., 2022). Given that RV infection disrupts the antioxidant system, the question remains whether RA can alleviate RV viral infection by modulating intestinal antioxidant capacity.

In conclusion, RA is a promising candidate for the development of novel therapeutics for the treatment of RV-induced intestinal damage. This study sheds light on the potential mechanisms underlying the beneficial effects of RA on regulating autophagy and oxidative homeostasis, and highlights the importance of exploring alternative therapeutic strategies for combating RV infections.

2. Materials and methods

2.1. Animal ethics statement

All experimental protocols were approved by the Institutional Animal Care and Use Committee of the Laboratory Animal Center at Sichuan Agricultural University (SICAU-2015-033).

2.2. Animal model and diet

In the current experiment, 36 Duroc × Landrace × Yorkshire (DLY) male piglets (from parity three and four sows) weaned at 21 d of age were randomly separated into 6 groups with 6 replicates per treatment, including a control group (treatment one), two concentration gradients of RA treatment (treatments two and three at 5 and 15 mg/d, respectively), an RV treatment group (treatment four), and two RV treatment groups supplemented with varying concentrations of RA (treatments five and six at 5 and 15 mg/d, respectively). The experiment lasted for a total of 25 d. On the d 21 of the experiment, the experimental pigs were weighed, orally administered $NaHCO_3$ (5 mL, 100 mmol/L), followed by oral administration of the RV inoculum at a dose of 8 mL (the OSU strain [G5P9; ATCC#VR-893], obtained from the National Veterinary Microorganism Culture Collection and Management Center, 2.8×10^9 PFU) for the infected group and sterile culture medium at the same volume for the control group. After RV inoculation, the diarrheal status of the piglets was recorded twice a day, piglets were sacrificed during the peak period of diarrhea. After collecting blood from piglets' hearts, 0.5-g liver and 2-cm samples from the jejunum were fixed in 4% paraformaldehyde for pathological analysis of the intestines. The remaining approximately 2 g of jejunum and liver tissue was then transferred to −80 °C for storage and further testing. The composition and nutrient levels of the basal diet are shown in Table 1 and the calculated nutrient levels were based on ingredient data of Nutrient Requirements of Swine (NRC, 2012).

2.3. Chemicals and reagents

RA (R2625, Sigma-Aldrich, St. Louis, MO, United States), pepstatin A (S7381, Selleckchem, Houston, TX, USA), aloxistatin (E64d) (S7393, Selleckchem, Houston, TX, USA), and rapamycin (S1039, Selleckchem, Houston, TX, USA) were used for the experiment.

2.4. Cell culture and viral infection

IPEC-J2 cells sourced from ATCC were cultured in DMEM/F12 medium supplemented with 10% fetal bovine serum (FBS), 100 IU/mL penicillin, 100 mg/mL streptomycin, 5 mg/mL human epidermal growth factor (hEGF), and 10 nM HEPES at 37 °C in a 5% CO_2 atmosphere incubator. Confluent IPEC-J2 cells (70%) were infected with RV at a multiplicity of infection (MOI) of 1 for 1 h at 37 °C. Non-adherent virus particles were removed and cells were washed once with PBS, followed by addition of fresh growth medium. IPEC-J2 cells were treated with RA (20 μM), pepstatin A (1 μM), BAF1 (5 μM) and rapamycin (1 μM), respectively, for 24 and 36 h. At the same time, RV was added in control, RA, BAF1 and rapamycin groups for 24 and 36 h.

Table 1
Composition and nutrient levels of the diet (%, dry-matter basis).

Ingredients	Content	Nutrient levels[3]	Content
Maize	29.32	DE, Mcal/kg	3.58
Extruded maize	28.00	CP	19.23
Extruded soymeal	6.00	Ca	0.72
Dehulled soybean meal	7.00	TP	0.60
Fish meal	5.00	AP	0.41
Low-protein milk whey	8.00	SID Lys	1.36
Soy protein concentrate	8.00	SID Met	0.46
Coconut oil	3.00	SID Met + Cys	0.73
Sugarcane	3.00	SID Thr	0.79
Limestone	0.40	SID Trp	0.22
Sodium chloride	0.30		
Choline	0.15		
Calcium phosphate	0.45		
L-Lys-HCL (78.8%)	0.45		
DL-Met	0.15		
L-Thr	0.12		
L-Trp	0.02		
Antioxidants	0.02		
Feed enzymes	0.10		
Vitamin premix[1]	0.32		
Mineral premix[2]	0.20		
Total	100.00		

DE = digestible energy; TP = total phosphorus; AP = available phosphorus; SID = standardized ileal digestible.
[1] The premix provides the following vitamins per kilogram of complete feed: vitamin D_3 1100 IU, vitamin E 32 IU, vitamin K_3 2.5 mg, biotin 250 μg, folic acid 1.5 mg, niacin 30 mg, vitamin B_1 5 mg, vitamin B_2 17.5 mg, vitamin B_6 14 mg, vitamin B_{12} 87 μg, pantothenic acid 15 mg.
[2] The premix provides the following minerals per kilogram of complete feed: iron ($FeSO_4 \cdot H_2O$), 100 mg; copper ($CuSO_4 \cdot 5H_2O$), 6 mg; manganese ($MnSO_4 \cdot H_2O$), 4 mg; zinc ($ZnSO_4 \cdot H_2O$), 100 mg; iodine (KI), 0.3 mg; selenium (Na_2SeO_3), 0.3 mg.
[3] The nutritional level of the feed is a calculated value.

Table 2
Primer sequences used in the study.

Gene name		Sequence (5′ to 3′)
β-Actin	Forward	GCTGTTTTCCCGTCCATTGT
	Reverse	ACAATGGACGGGAAAACAGC
Aldh1a1	Forward	TGTGTGGCCAGATCATTCCT
	Reverse	AGGAATGATCTGGCCACACA
Aldh1a2	Forward	AACCGTTCCTGCAAGCTTTT
	Reverse	AAAAGCTTGCAGGAACGGTT
Aldh1a3	Forward	TAAAGAAGCTGCCTCCCGAA
	Reverse	TTCGGGAGGCAGCTTCTTTA
CYP26	Forward	AAGGACTACTCGGATGCTCTGGA
	Reverse	CTTCAGCTCCTGCATGGTCATCTC
HAMP	Forward	AAGACAGCTCACAGACCTCC
	Reverse	ATCCCACAGATTGCTTTGCG
SOX9	Forward	CTCCCAACGCCATCTTCAAG
	Reverse	CTTGAAGATGGCGTTGGGAG
HES1	Forward	GAGTGCATGAACGAGGTGAC
	Reverse	CGTTGATCTGGGTCATGCAG
NOTCH1	Forward	CTGCGAGGAGAACATTGACG
	Reverse	CGTCAATGTTCTCCTCGCAG
CGA	Forward	TGCCCCAATCTATCAGTGCA
	Reverse	TGCACTGATAGATTGGGGCA
OLFM4	Forward	CAAGATGTGGCTGGGTTTCC
	Reverse	GGAAACCCAGCCACATCTTG
Occludin	Forward	ATCCTGGGTGTGATGGTGTT
	Reverse	TGAGTGCTATCCTGGGTGTG
Claudin-1	Forward	TGAACACCACTTTGCAAGCA
	Reverse	TCAGATTCAGCAAGGAGTCGA

Aldh1a1 = aldehyde dehydrogenase 1 family member A1; *Aldh1a2* = aldehyde dehydrogenase 1 family member A2; *Aldh1a3* = aldehyde dehydrogenase 1 family member A3; *CYP26* = cytochrome P450 family 26; *HAMP* = hepcidin antimicrobial peptide; *SOX9* = SRY-box transcription factor 9; *HES1* = hairy and enhancer of split 1; *NOTCH1* = Notch receptor 1; *CGA* = chlorogenic acid; *OLFM4* = olfactomedin 4.

2.5. Histological analysis, immunofluorescence

The intestinal tissue was harvested and fixed in 4% paraformaldehyde in PBS overnight before being embedded in paraffin. The 5-μm sections were stained with hematoxylin and eosin (H&E) for histological analysis and for RV protein detection. Samples were also embedded in optimal cutting temperature (OCT), and 8-μm sections were used for immunofluorescence staining with primary antibodies, including the RV capsid antibody (sc-101363, Santa Cruz, Dallas, Texas, USA) at a 1:100 dilution. Secondary antibodies, goat anti-mouse IgG Alexa Fluor 488 (ab150113, Abcam, Cambridge, UK), were applied at dilutions of 1:500 to 1:1000.

2.6. qPCR and Western blotting

RNA samples from tissues or cells were extracted using the TRIzol reagent (15596026, Invitrogen, Massachusetts, USA) and normalized to a concentration of 1 μg/μL, following the manufacturer's instructions. The reverse transcription reaction was set up according to the instructions provided with the Reverse Transcription Kit (RR037A, Takara, Chuo-ku, Tokyo, Japan). The relative gene expression was calculated using the ΔΔCT method and normalized to the housekeeping gene β-actin. The primer sequences are shown in Table 2.

Western blotting was conducted as previously described (Wu et al., 2020) using primary antibodies against zonula occludens-1 (ZO-1) (13663, Cell Signaling Technology, Danvers, MA, USA), occludin (911131, Cell Signaling Technology, Danvers, MA, USA), claudin-1 (13255, Cell Signaling Technology, Danvers, MA, USA), pNRF2 (ab76026, Abcam, Cambridge, UK), NRF2 (16396-1-AP, Proteintech, Wuhan, China), heme oxygenase 1 (HO-1) (10701-1-AP, Proteintech, Wuhan, China), sequestosome 1 (p62) (ab56416, Abcam, Cambridge, UK), glutathione peroxidase 4 (GPX4) (ab125066, Abcam, Cambridge, UK), Unc51-like kinase 1 (ULK1) (8054, Cell Signaling Technology, Danvers, MA, USA), pULK1 (14202, Cell Signaling Technology, Danvers, MA, USA), autophagy-related gene (ATG) 7 (8558, Cell Signaling Technology, Danvers, MA, USA), ATG16 (8089, Cell Signaling Technology, Danvers, MA, USA), ATG14 (96752, Cell Signaling Technology, Danvers, MA, USA), coiled-coil, moesin-like BCL2-interacting protein (Beclin) (3495, Cell Signaling Technology, Danvers, MA, USA), pBeclin (14717, Cell Signaling Technology, Danvers, MA, USA), ATG5 (9980, Cell Signaling Technology, Danvers, MA, USA), ATG3 (3415, Cell Signaling Technology, Danvers, MA, USA), syntaxin (2869, Cell Signaling Technology, Danvers, MA, USA), synaptosome associated protein 29 (SNAP29) (sc-390602, Santa Cruz, Dallas, Texas, USA), RAS-related protein Rab-7a (RAB7A) (9367, Cell Signaling Technology, Danvers, MA, USA), LC3I/II (4108, Cell Signaling Technology, Danvers, MA, USA), and β-actin (3700, Cell Signaling Technology, Danvers, MA, USA). The primary antibodies were diluted 1:1000. Secondary goat anti-rabbit and goat anti-mouse antibodies conjugated with HRP (sc-2030 and sc-2031, Santa Cruz, Dallas, Texas, USA) were diluted to a concentration of 1:3000.

2.7. Measurement of GSH, malondialdehyde (MDA), glutathione peroxidase (GSH-PX), superoxide dismutase (SOD), catalase (CAT) and hydroxyl radical (·OH) levels

Assay kits for reduced GSH (A006-2-1), lipid peroxidation MDA (S0131M), GSH-PX (A005-20-1), SOD (A001-3-2), CAT (A007-1-1), and ·OH (A018-1-1) were obtained from Nanjing Jiancheng Bioengineering Institute, Nanjing, China and were used according to the manufacturer's instructions to measure intracellular GSH and MDA levels.

2.8. Statistical analysis

Statistical analyses were carried out using Microsoft Excel software and GraphPad Prism and all data are expressed as mean ± SD. Unpaired two-tailed Student's *t*-test and/or one-way ANOVA were used to compared groups. *P*-values between 0.05 and 0.10 were considered to have significant trends ($0.05 < P < 0.10$) and $P < 0.05$ was taken as statistically significant ($^{*}P < 0.05$, $^{**}P < 0.01$, $^{***}P < 0.001$ and $^{****}P < 0.0001$). All results were plotted using GraphPad Prism 7 software.

3. Results

3.1. Development of an oral model for RV challenge and the evaluation of the effects of RA supplementation

After exposure to RV, we examined the jejunum morphology with H&E stains in both the control and RV-challenged groups. Compared with control, there were significant decrease in villus architectures in RV-treated group in (Fig. 1A). Experimental flow, design and the concentration of oral RV challenge are indicated in Fig. 1B. To assess the absorption and metabolism of RA, the gene expression of key regulators aldehyde dehydrogenase 1 family member A1 (*Aldh1a1*), aldehyde dehydrogenase 1 family member A2 (*Aldh1a2*), and aldehyde dehydrogenase 1 family member A3 (*Aldh1a3*), which are crucial aldehyde dehydrogenase isozymes involved in the irreversible oxidation of retinaldehyde for RA synthesis, as well as cytochrome P450 family 26 (*CYP26*), a metabolic enzyme that plays a critical role in RA degradation, were measured. The results presented in Fig. 1C and D showed that *CYP26* gene expression significantly increased in the RA-treated groups in both liver and jejunum ($P < 0.05$), indicating the effectiveness of oral RA supplementation and RA overload in the treated groups. The findings on the expression of aldehyde dehydrogenase isozymes, however, showed contradicting results in liver and jejunal tissues. Specifically, in the liver, significant upregulation of *Aldh1a1*, *Aldh1a2*, and *Aldh1a3* was observed in the 15 mg/d-RA group ($P < 0.05$), whereas in the jejunum, surprisingly significant downregulation of *Aldh1a2* and *Aldh1a3* was found ($P < 0.05$), which may indicate negative feedback regulation. These results demonstrated the effectiveness of both oral RV challenge and RA supplementation in the study.

3.2. RA alleviated RV-induced disruption in intestinal architecture and signaling

Studies have shown that RV-induced intestinal damage is mediated by several mechanisms, including oxidative stress, proinflammatory cytokines, and disruption of the intestinal barrier function (Baker and Prasad, 2010). Our histological analysis of the jejunum using H&E staining revealed that RV infection led to extensive damage to the intestinal architecture. However, treatment with RA appeared to mitigate this damage, as evidenced by the restoration of both the villus and crypt structure (Fig. 1E). To further investigate the morphological changes in the intestine, we performed a statistical analysis. The results showed that RA treatment alone increased the villus height in both the 5 mg/d and 15 mg/d groups ($P < 0.05$), and only affected the villus height/crypt depth ratio in the low-dose group (Table 3; $P < 0.05$). In the RV-challenged group, there was a numerical but non-significant decrease in villus height and crypt depth ($P > 0.05$). However, treatment with low doses of RA in the RV group resulted in a significant increase in both villus height and the villus height/crypt depth ratio ($P < 0.05$). The mRNA expression of SRY-box transcription factor 9 (*SOX9*), a crucial transcription factor for epithelial regeneration, and olfactomedin 4 (*OLFM4*), a marker for intestinal stem cells (ISC), significantly decreased in RV-challenged groups but significantly increased in groups treated with RA ($P < 0.05$), as illustrated in Fig. 1F. These observations indicated compromised ISC signaling in RV-challenged groups, but recovery with RA treatment. Notch receptor 1 (Notch1) and hairy and enhancer of split 1 (HES1) are both involved in ISC signaling. HES1 is a Notch target gene that plays a role in cell fate decisions and differentiation processes within the intestinal epithelium. HES1 represses the basic helix-loop-helix transcription factor Math1, and HES1 deficiency leads to increased Paneth, goblet, and enteroendocrine cells in the intestine (Pellegrinet et al., 2011). Concordant with the results, both *HES1* and *Notch1* gene expression significantly increased in RV-challenged groups with both RA treatment ($P < 0.05$) except for 5 mg/d RA in *HES1* ($P = 0.091$), suggesting that RA can enhance Notch signaling in piglets' jejunum. Moreover, the gene expression of chlorogenic acid (*CGA*), a marker for enteroendocrine cells that maintain intestinal homeostasis and function, significantly increased in RA-treated groups without RV infection, only had a recovery tendency in 15 mg/d RA group after RV challenge ($P = 0.060$), as demonstrated in Fig. 1F. In addition, 15 mg/kg RA in RV-treated group significantly promoted occludin gene expression ($P < 0.05$). Compared with control, RV challenge had the tendency to decrease claudin-1 gene expression ($P = 0.064$), but it was recovered by 5 mg/kg RA supplementation ($P = 0.060$).

Next, we assessed protein expression in both RA-treated alone group and RV-challenged groups supplemented with two-dose RA groups. The data presented in Fig. 1G and I demonstrated that 15 mg/d RA supplementation significantly upregulated ZO-1 ($P < 0.05$) and claudin-1 expression ($P = 0.069$). In addition, 5 mg/d RA significantly increased claudin-1 expression ($P < 0.01$). However, there was a significant decrease in occludin protein expression in 15 mg/d ($P < 0.05$), which differed with the results in occludin gene expression. RA supplementation reversed the RV-induced claudin-1 decrease in both 5 mg/d and 15 mg/d groups ($P < 0.05$), while only exhibiting a tendency to increase occludin protein expression in the 5 mg/d RA group against RV challenge ($P = 0.070$), as shown in Fig. 1H and J. However, although RA could enhance ZO-1 protein expression when supplemented alone, it could not induce ZO-1 upregulation in the case of RV challenge ($P > 0.05$). Taken together, these findings imply that RA can safeguard the intestinal structure from damage in the scenario of RV challenge.

3.3. Effects of RA on anti-oxidative signaling and redox homeostasis after RV challenge

NRF2 and HO-1 play crucial roles in maintaining redox homeostasis (Xiang et al., 2022). NRF2 is a transcription factor that activates genes involved in oxidative stress response and detoxification (He et al., 2020). Activation of NRF2 and its dependent genes, including HO-1, glutamate-cysteine ligase catalytic subunit (GCLC), and NAD(P)H:quinone oxidoreductase 1 (NQO1), help maintain cellular redox equilibrium (Gambhir et al., 2022). Our findings suggest that RA alone can significantly increase the pNRF2 to NRF2 ratio in the high-dose group ($P < 0.05$) and enhance HO-1 protein expression in both concentration groups ($P < 0.05$). However, GPX4 protein expression, which plays a crucial role in preventing lipid peroxidation, did not appear to change significantly ($P > 0.05$) (Fig. 2A, C, D, and E). Furthermore, RV challenge led to decreased pNRF2 to NRF2 ratio and HO-1 protein expression ($P < 0.01$), but had no effect on GPX4 expression ($P > 0.05$). Interestingly, when RA was supplemented in RV groups, the protein expression of pNRF2 to NRF2 ratio was restored, 15 mg/d RA ($P < 0.01$) and 5 mg/RA ($P = 0.054$). In addition, the protein expression of HO-1 was

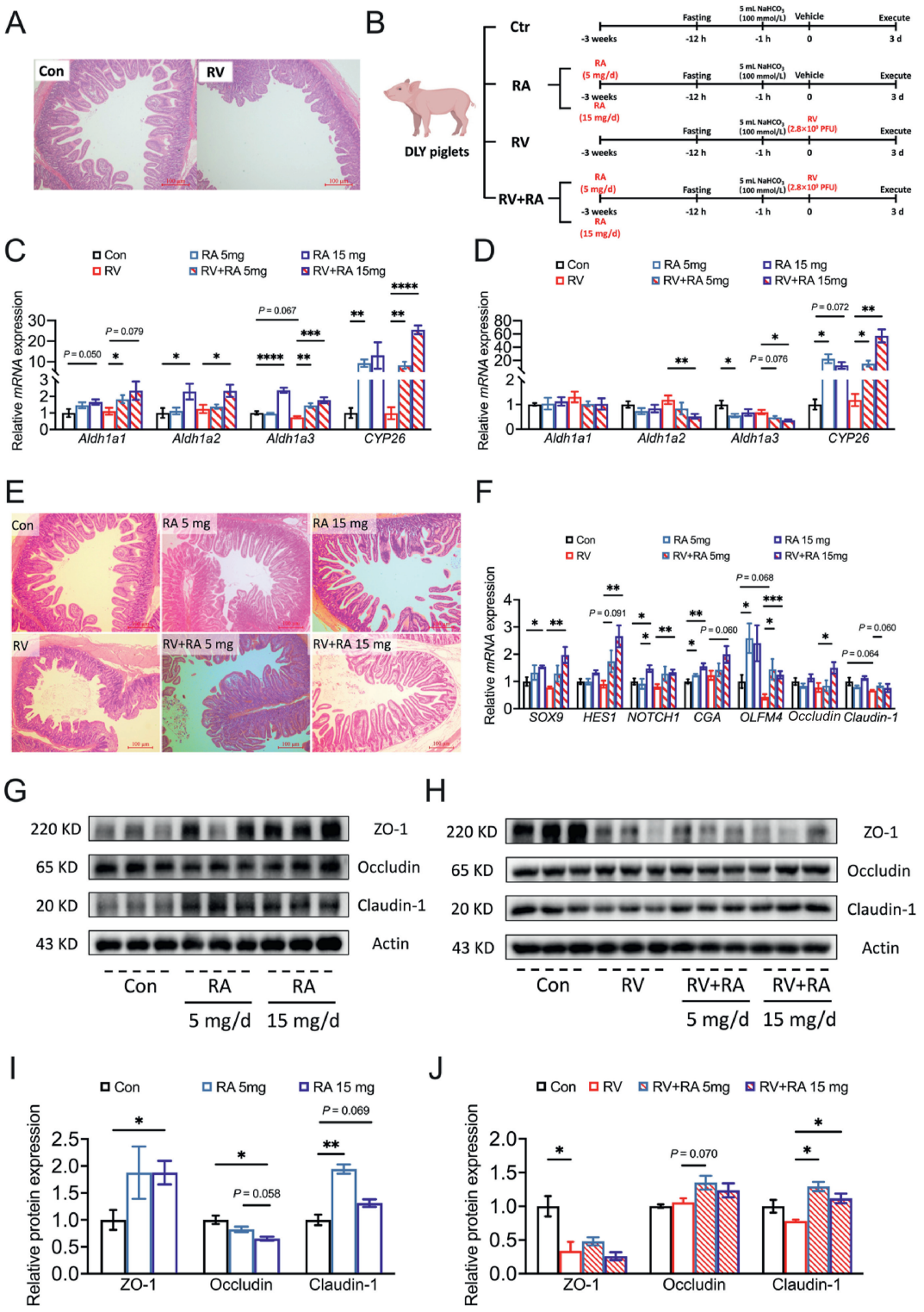

Fig. 1. Effects of retinoic acid (RA) on intestinal architecture and signaling after rotavirus (RV) challenge. (A) Hematoxylin and eosin (H&E) staining of control and RV-challenged groups. Scale bar = 100 μm. (B) The experimental flow and the concentration of RV and RA. (C and D) The mRNA expression of *Aldh1A1*, *Aldh1A2*, and *Aldh1A3* and *CYP26* in liver and jejunum ($n = 6$). (E) H&E staining of the villus and crypt in jejunum ($n = 6$). Scale bar = 100 μm. (F) Gene expression analysis of intestinal stem cell signaling and barrier related genes (*SOX9*, *HES1*, *NOTCH1*, *CGA*, *OLFM4*, occludin and claudin-1) ($n = 6$). (G and I) Protein expressions and grayscale analysis of intestinal barrier related proteins in RA-treated groups ($n = 3$). (H and J) Protein expressions and grayscale analysis of intestinal barrier related proteins were performed in RV-challenged groups supplemented with RA ($n = 3$). KD = kiloDalton; *Aldh1a1* = aldehyde dehydrogenase 1 family member A1; *Aldh1a2* = aldehyde dehydrogenase 1 family member A2; *Aldh1a3* = aldehyde dehydrogenase 1 family member A3; *CYP26* = cytochrome P450 family 26; *SOX9* = SRY-box transcription factor 9; *HES1* = hairy and enhancer of split 1; *NOTCH1* = Notch receptor 1; *CGA* = chlorogenic acid; *OLFM4* = olfactomedin 4. *$P < 0.05$, **$P < 0.01$, ***$P < 0.001$ and ****$P < 0.0001$.

Table 3
Effects of retinoic acid (RA) on intestinal architecture of the jejunum after rotavirus (RV) challenge.

Item	Intestine architecture		
	Villus height, μm	Crypt depth, μm	Villus height/crypt depth
Con	177.57 ± 9.21^{AB}	115.70 ± 5.09^{AB}	1.54 ± 0.08^{AB}
RA 5 mg	150.43 ± 13.06^{A}	139.88 ± 11.96^{B}	1.10 ± 0.10^{A}
RA 15 mg	262.78 ± 20.32^{C}	108.30 ± 9.47^{AB}	2.47 ± 0.17^{CD}
RV	194.72 ± 10.20^{B}	135.25 ± 8.12^{AB}	1.49 ± 0.18^{AB}
RV + RA 5 mg	282.03 ± 13.53^{C}	106.27 ± 9.32^{A}	2.81 ± 0.37^{D}
RV + RA 15 mg	241.55 ± 13.53^{C}	128.58 ± 14.07^{AB}	1.98 ± 0.21^{BC}
P-values			
RV challenge effects	0.000	0.592	0.000
RA treatment effects	0.000	0.006	0.000
RV × RA interaction effect	0.331	0.974	0.422

$^{A-C}$Different letters represent significant differences at $P \leq 0.05$.

promoted in RV-treated piglets after orally administration of 15 mg/d RA ($P = 0.062$) and 5 mg/d RA ($P < 0.01$) (Fig. 2B, F, G, and H). GSH and MDA are essential for maintaining redox homeostasis. While GSH acts as a redox buffer, an antioxidant, and an enzyme cofactor against oxidative stress, MDA reflects the degree of cellular injury and senescence (Aoyama and Nakaki, 2015). Our study demonstrated that MDA levels significantly increased in RV challenged groups but decreased in the high-dose RA treated group ($P < 0.01$) (Fig. 2I). GSH levels also significantly increased in the high-dose RA treated groups, both in non-RV and RV challenged groups ($P < 0.05$) (Fig. 2J). However, there were no noticeable changes in GSH-PX levels ($P > 0.05$) (Fig. 2K). SOD and CAT are responsible for reducing reactive oxygen species (ROS), including superoxide anion ($O_2^{-\cdot}$) and hydrogen peroxide (H_2O_2), to maintain a balance between ROS production and elimination in cells (Das and Roychoudhury, 2014; Nadarajah, 2020). Our data showed that at the higher dosage (15 mg/d), RA significantly increased SOD and CAT levels in both RV or non-RV situations ($P < 0.05$), while at the lower dosage, it only elevated SOD levels significantly without RV challenge, and CAT levels in RV challenge scenarios ($P < 0.05$) (Fig. 2L and M). Surprisingly, RA supplementation significantly increased ·OH levels in the low-dose context ($P < 0.05$), and there were no noticeable changes in RV challenges (Fig. 2N). These findings suggest that RA may play a potential role in regulating redox homeostasis against RV challenges through its ability to activate the NRF2/HO-1 signaling pathway, along with other enzymatic components.

3.4. RA supplementation promoted autophagy initiation but impaired autophagic degradation in piglet's jejunum

Since RV infection has complex effects on autophagy, including induction of LC3 lipidation and viroplasm formation, suppression of autophagy maturation, and modulation of autophagy pathways via the PI3K-Akt-mTOR axis. Therefore, we aimed to investigate whether RA could regulate autophagy-related pathways. We measured the levels of essential autophagy-associated proteins and classified the results into three parts. Firstly, RA treatment significantly increased the pBeclin to Beclin ratio ($P < 0.05$), indicating the promotion of autophagy initiation (Fig. 3A and F). In line with these findings, we observed a significant increase in the p-ULK1/ULK1 ratio in the RA-treated group ($P < 0.05$), indicating enhanced autophagy initiation and autophagosome formation (Fig. 3A and E). Secondly, we found that there were no significant changes in ATG16, ATG14, and ATG3 protein levels in the RA group ($P > 0.05$), but we did observe a significant promotion of ATG7 ($P < 0.05$) and ATG5 (5 mg/d RA, $P = 0.069$) protein expression, which stimulated autophagosome formation (Fig. 3C and G). Thirdly, our results on autophagosome-lysosome fusion were contradictory. While syntaxin and SNAP29 were increased in the 5 mg/d RA group ($P < 0.05$), RAB7A protein level decreased significantly in the 5 mg/d RA group ($P < 0.05$) and showed a reduction tendency in the 15 mg/d group ($P = 0.078$) (Fig. 3G). Additionally, both p62 and the LC3-II to LC3-I ratio increased significantly in the high-dose RA group ($P < 0.05$), indicating the accumulation of autophagy substrates due to impaired autophagic degradation and flux (Fig. 3G and H). Taken together, our data suggest that RA may promote autophagy initiation, but can also indicate a blockage or impairment in the autophagic process that prevents the completion of autophagic degradation.

3.5. RA had potential to alleviate RV infection-induced autophagic alterations

In our preliminary experiments, we observed that RA can modulate cellular autophagy. Therefore, we used immunofluorescence-based quantification to investigate the effect of RA supplementation on the RV infection rate in the porcine jejunum (red dots indicate RV protein staining). As shown in Fig. 4A, there was no apparent RV fluorescence in the control and RA-treated groups. In contrast, the RV challenged group exhibited a large amount of red fluorescence, while RA supplementation appeared to decrease the level of RV infection (Fig. 4A). Next, we used Western blotting to analyze the expression of autophagy-related proteins in the RV-infected and RV-infected with RA-treated groups. Our findings reveal that RV infection markedly decreased pBeclin to total ratios ($P < 0.05$). However, the introduction of high doses of RA substantially recovered the pBeclin and total protein ratios ($P < 0.05$) (Fig. 4A and F). In addition, RV infection significantly reduced the pULK1 to total protein ratio ($P < 0.01$), while the RA at the high-dose level greatly alleviated the decrease in pULK1 levels caused by RV infection ($P < 0.01$) (Fig. 4A and E). This suggests that RA can reduce RV-induced autophagy suppression. Furthermore, ATG7 and ATG16 protein expression were significantly reduced by RV infection ($P < 0.05$), but RA administration restored ATG7 protein expression levels ($P < 0.05$) and had the tendency to enhance ATG16 protein levels ($0.05 < P < 0.10$). ATG14 protein expression was not significantly affected by RV infection ($P > 0.05$), but at the high-dose level, RA increased its expression compared to the RV-treated group ($P < 0.05$) (Fig. 4H). Only the low-dose RA treatment significantly increased ATG3 expression compared to the RV-infected group ($P < 0.05$) (Fig. 4I). Interestingly, the autophagosome fusion-related proteins syntaxin, SNAP29, and RAB7A did not exhibit the same results as the RA-alone group. The addition of a high-dose of RA significantly reduced syntaxin expression in the RV-infected group ($P < 0.05$), while at the low-dose level, RA significantly increased SNAP29 expression compared to the

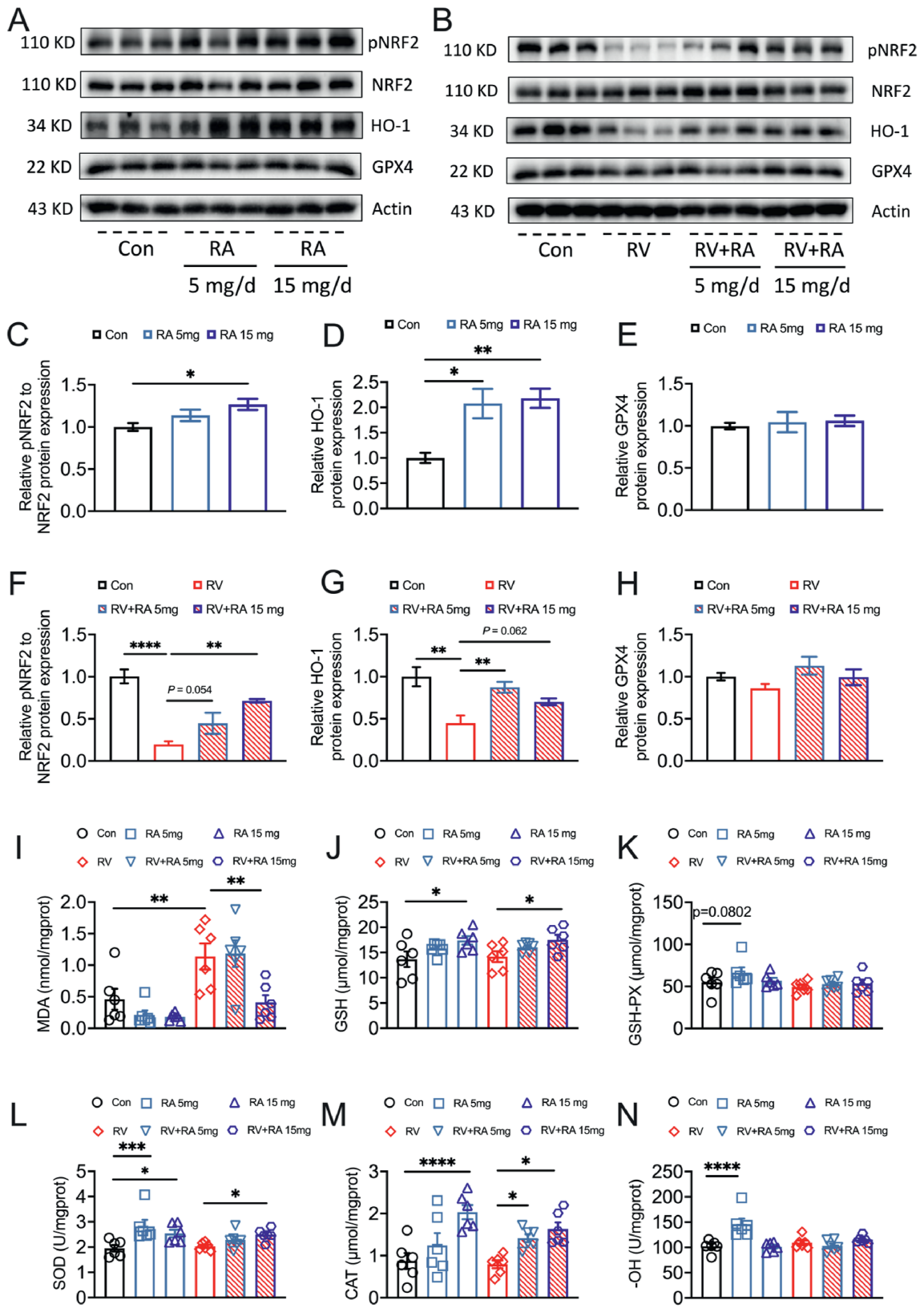

Fig. 2. Effects of retinoic acid (RA) on anti-oxidative signaling and redox homeostasis after rotavirus (RV) challenge. (A and B) Western blotting analysis of anti-oxidative related proteins (pNRF2, NRF2, HO-1 and GPX4) in high and low dose RA treatment groups and the high and low dose RA treatment groups with RV challenge ($n = 3$). (C to H) Grayscale analysis of redox homeostasis related proteins were performed in RA-treated groups and RV-challenged groups supplemented with RA ($n = 3$). (I to N) Redox homeostasis-relative enzymatic activity were analyzed, including MDA, GSH, GSH-PX, SOD, CAT and ·OH ($n = 6$). KD = kiloDalton; NRF2 = nuclear factor erythroid 2-related factor 2; HO-1 = heme oxygenase 1; GPX4 = glutathione peroxidase 4; MDA = malondialdehyde; GSH = glutathione; GSH-PX = glutathione peroxidase; SOD = superoxide dismutase; CAT = catalase; ·OH = hydroxyl radical. *$P < 0.05$, **$P < 0.01$, ***$P < 0.001$ and ****$P < 0.0001$.

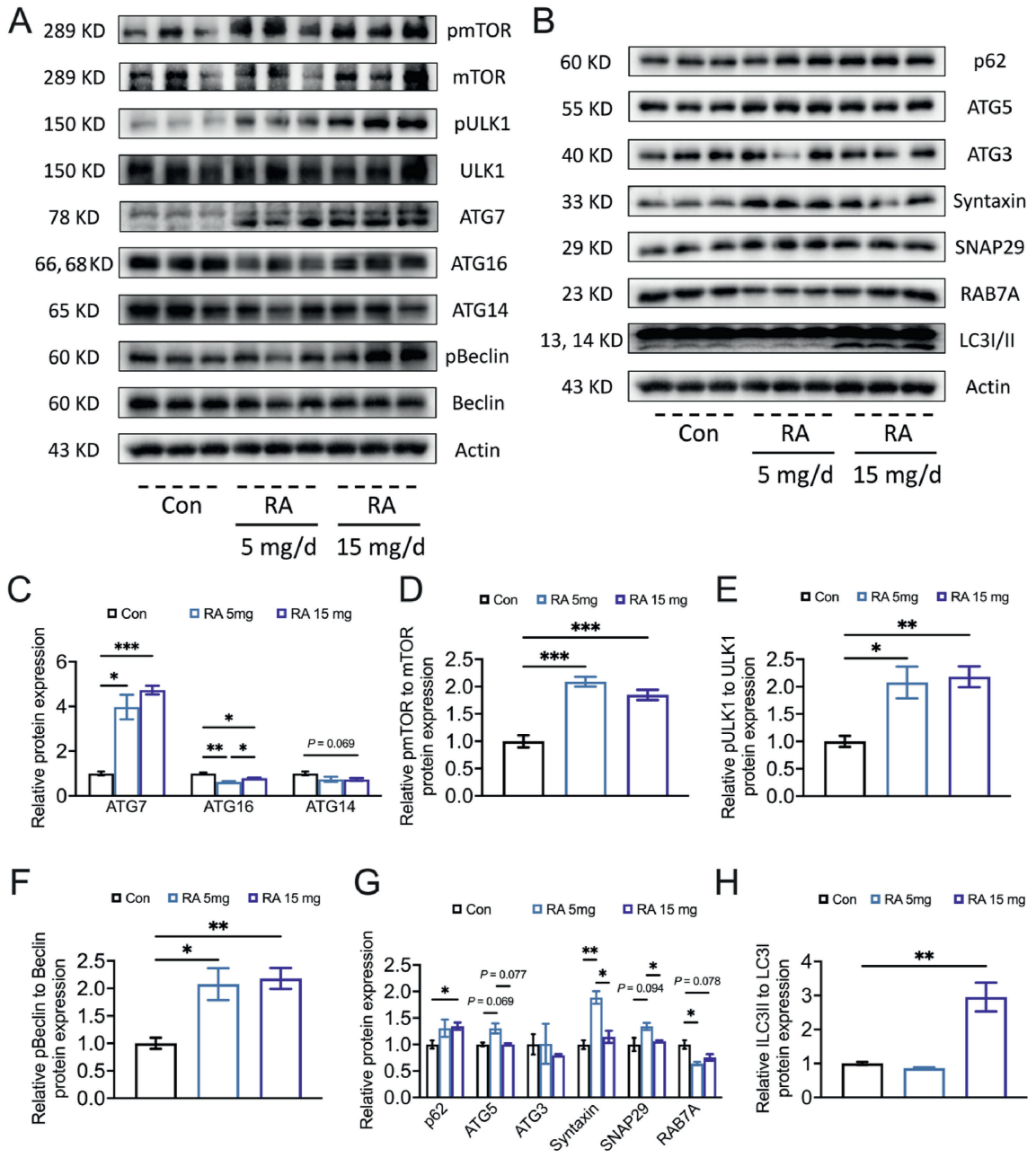

Fig. 3. Effects of retinoic acid (RA) administration on autophagy activation in jejunum from control and RA-treated groups. (A and B) Western blotting analysis of autophagy-related proteins including autophagy induction and regulation (pBeclin/Beclin, pULK1/ULK1, ATG7, ATG16 and ATG14), autophagy cargo recognition and degradation (p62, ATG5, ATG3), and autophagy maturation and lysosomal fusion (syntaxin, SNAP29, Rab7A and LC3I/II) ($n = 3$). (C to G) Gray value analysis of the above protein expressions ($n = 3$). KD = kiloDalton; Beclin = coiled-coil, moesin-like BCL2-interacting protein; ULK1 = Unc51-like kinase 1; ATG = autophagy-related gene; p62 = sequestosome 1; SNAP29 = synaptosome associated protein 29; RAB7A = RAS-related protein Rab-7a; LC3 = microtubule-associated protein light chain 3. *$P < 0.05$, **$P < 0.01$ and ***$P < 0.001$.

RV-infected group ($P < 0.05$). RAB7A expression showed a trend towards increased expression after the addition of RA following RV infection ($P = 0.055$) (Fig. 4I). Finally, we observed that both p62 and LC3-II/I were decreased in intestinal epithelial cells under RV infection (p62 was significantly reduced ($P < 0.05$), and LC3-II/I showed a trend ($P = 0.067$)), indicating a reduction in the overall autophagy activity within the cell. Upon addition of RA, both p62 and LC3-II/I were completely restored to levels seen in non-infected cells (Fig. 4C, G and I). These experiments suggest that RA can alleviate RV-induced regulation of cellular autophagy, which may be a mechanism to combat RV infection.

3.6. Autophagy activation and impaired autophagic flux reduced RV infection in IPEC-J2 cells

To investigate the role of RA in autophagy and its mechanism in alleviating RV infection, we employed porcine intestinal epithelial cells (IPEC-J2) as a model. Treatment with RA for 24 and 36 h resulted in protein changes that were consistent with those observed in vivo: the ratio of p-ULK1 to ULK1 increased, indicating that RA may enhance autophagy levels in intestinal cells. Furthermore, the cells exhibited significant accumulation of both p62 and LC3-II, indicating that autophagic flux was blocked while

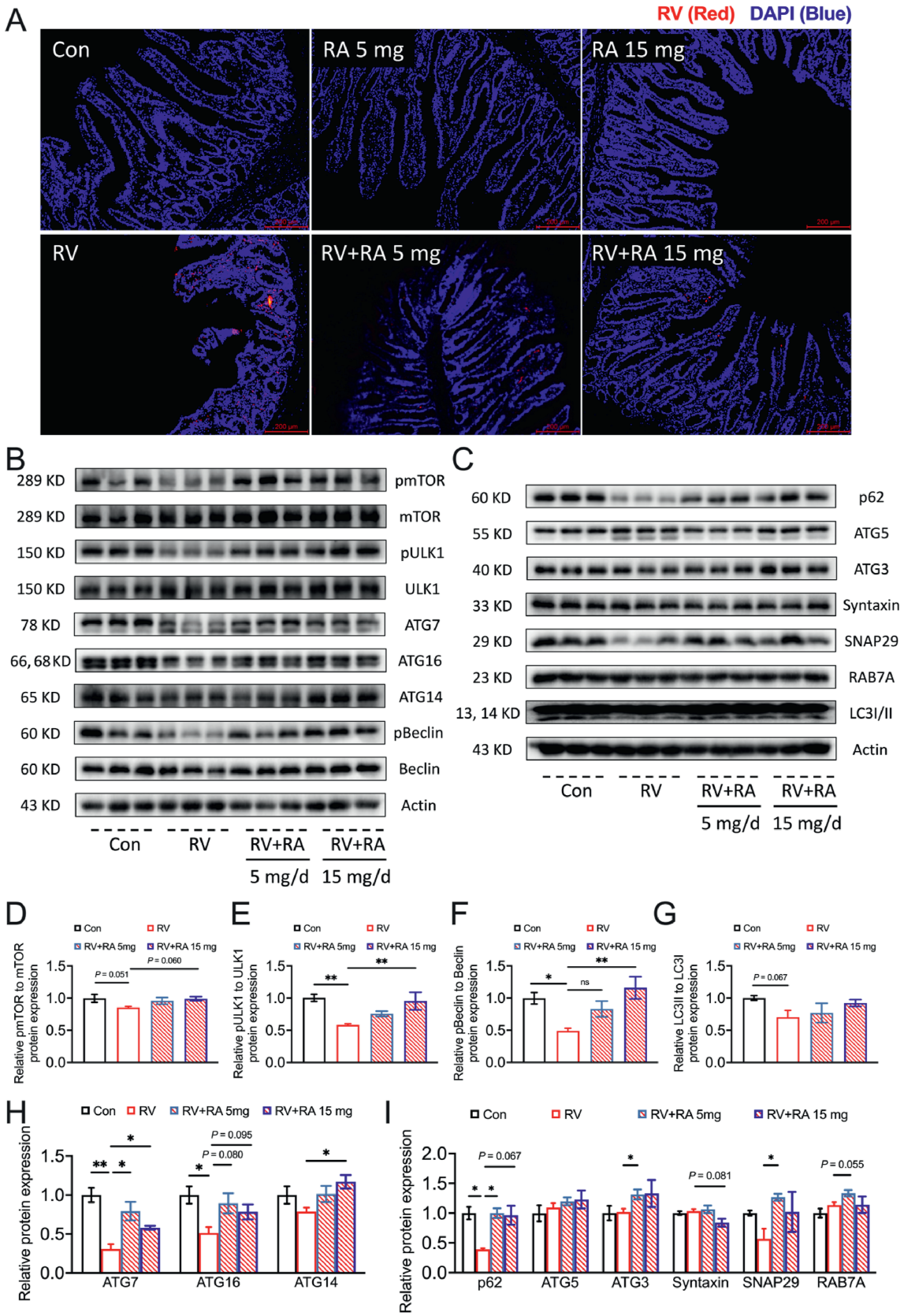

Fig. 4. Effects of retinoic acid (RA) administration on regulating autophagic pathways in jejunum from control, rotavirus (RV) and RV + RA groups. (A) Fluorescence density of RV in all six treatment groups in jejunum sample (red fluorescence indicates RV protein detection). Scale bar = 200 μm. (B and C) Western blotting analysis of autophagy-related proteins including autophagy induction and regulation (pBeclin/Beclin, pULK1/ULK1, ATG7, ATG16 and ATG14), autophagy cargo recognition and degradation (p62, ATG5 and ATG3), and autophagy maturation and lysosomal fusion (syntaxin, SNAP29, RAB7A and LC3I/II) ($n = 3$). (D to I) Gray value analysis of the above protein expressions ($n = 3$). KD = kiloDalton; Beclin = coiled-coil, moesin-like BCL2-interacting protein; ULK1 = Unc51-like kinase 1; ATG = autophagy-related gene; p62 = sequestosome 1; SNAP29 = synaptosome associated protein 29; RAB7A = RAS-related protein Rab-7a; LC3 = microtubule-associated protein light chain 3. *$P < 0.05$, and **$P < 0.01$.

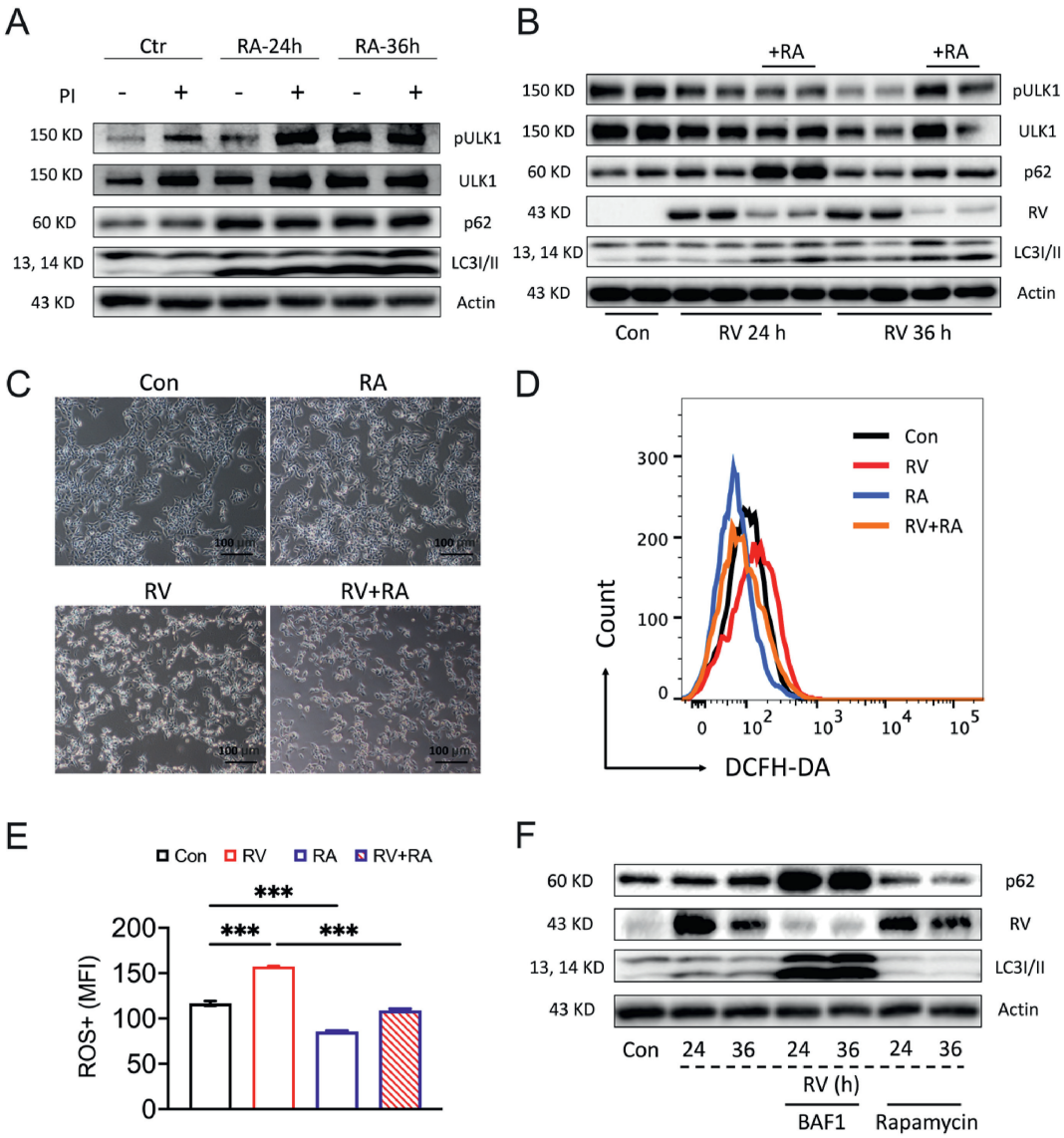

Fig. 5. Activation of autophagy and subsequent impairment of autophagic flux reduced RV infection in porcine jejunum cells (IPEC-J2). IPEC-J2 cells were treated with retinoic acid (RA; 20 μM), pepstatin A (1 μM), BAF1 (5 μM) and rapamycin (1 μM), respectively, for 24 and 36 h. At the same time, rotavirus (RV; MOI = 1) was added in control, RA, BAF1 and rapamycin groups for 24 and 36 h. (A) Western blotting analysis of autophagic flux-related proteins (p62 and the ratio of LC3-II to LC3-I) in RA-treated cells ($n = 1$) and autophagy initiation-related proteins (pULK1/ULK1) ($n = 1$). (B) Western blotting analysis of RA supplementation on pULK1, ULK1, p62, RV and LC3I/II protein expression after RV infection. (C) Microscopic observations of RV infected IPEC-J2 cells supplemented with RA. Scale bar = 100 μm. (D and E) ROS level in RV infected IPEC-J2 cells supplemented with RA ($n = 3$). (F) Western blotting analysis of autophagic flux-related proteins (p62 and the ratio of LC3-II to LC3-I) as well as RV protein expression in RV infection, BAF1 and rapamycin-treated cells ($n = 2$). KD = kiloDalton; ULK1 = Unc51-like kinase 1; p62 = sequestosome 1; LC3 = microtubule-associated protein light chain 3; ROS = reactive oxygen species; MFI = median fluorescence intensity. ***$P < 0.001$.

autophagy levels were increased (Fig. 5A). Pepstatin A (PI, autophagic flux inhibitor) treatment did not further increase the accumulation of p62 and LC3-II, indicating that RA effectively blocked autophagic flux (Fig. 5A). Further experiments revealed that RA reduces the RV protein expression at 24 and 36 h by modulating the key autophagy-related proteins p62 and LC3-II (Fig. 5B). Microscopic observations also indicated that RA partially mitigates the morphological changes in IPEC-J2 cells caused by RV infection when compared to the RV-infected group (Fig. 5C). In our investigation on piglets, we observed that RA regulates intestinal redox homeostasis. Subsequently, we assessed cellular ROS levels and results demonstrated a significant increase in cellular ROS levels in the RV-infected control group, whereas RA supplementation alone significantly decreased ROS levels. Moreover, the addition of RA to the RV-infected group substantially reduced RV-induced ROS accumulation (Fig. 5D and E). Last, to elucidate whether RA inhibits RV infection by increasing autophagy levels or inhibiting autophagic flux, we treated IPEC-J2 cells with E64d (a commonly used autophagic flux inhibitor) and rapamycin (a commonly used autophagic activator). We found that both E64d and RA had similar effects on inhibiting autophagic flux in RV-infected cells, significantly increasing the accumulation of p62 and LC3-II in the cytoplasm and inhibiting RV expression. Conversely, rapamycin increased autophagic flux (as indicated by decreased p62 and LC3-II levels) but did not significantly inhibit RV expression (Fig. 5F). These results suggest that inhibiting autophagic flux can effectively suppress RV infection and replication, while enhancing autophagy levels does not have a significant inhibitory effect on RV infection.

4. Discussion

RV is the major cause of pediatric diarrhea worldwide, resulting in a significant number of deaths annually, particularly in low- and middle-income countries. Live-attenuated oral vaccines for RV have shown reduced efficacy in these countries (Tohmé and Delgui, 2021). Despite the global introduction of vaccinations for RV over a decade ago, RV infections remain a leading cause of severe, dehydrating gastroenteritis in children under 5 years of age. In the pig industry, RV is an emerging pathogen and now recognized as the primary cause of gastroenteritis in neonatal piglets, leading to significant economic losses (Guo et al., 2022). Therefore, it is crucial to find strategies to alleviate RV-induced intestinal damages.

Research with rat models has revealed that intestinal crypt epithelial stem cells exhibited elevated aldehyde dehydrogenase (ALDH) levels in humans (Bose and Sarma, 1975; Huang et al., 2009), possess the highest concentration of RA (Thomas et al., 2005). This indicates a potential significance of crypt stem cells in the production of intestinal RA. Another research found that RA improves incidence and severity of necrotizing enterocolitis by repopulation of $LGR5^{+}$ ISC (Niño et al., 2017). The current findings provide compelling evidence that RA supplementation exerts a protective effect against RV-induced damage to the intestinal architecture and signaling. One of the key observations from our study is the restoration of the villus and crypt structure in response to RA supplementation. To gain insights into the underlying mechanisms of RA's beneficial effects, we assessed mRNA expression of *SOX9* and *OLFM4*, which serve as markers for ISC (Baker and Prasad, 2010). In the RV-challenged groups, the expression of *SOX9* and *OLFM4* was compromised, indicating an impairment of the intestinal stem cell population. However, RA administration effectively restored the expression of these markers, emphasizing the regenerative potential of RA in supporting intestinal stem cell function. Moreover, a previous experiment showed RA plays a crucial role in intestinal barrier protection and the maintenance of epithelial integrity (Yamada and Kanda, 2019). The findings were consistent with another research which showed that β-carotene (a provitamin A carotenoid) positively affects growth performance and intestinal morphology (Cheng et al., 2021). In our study, intestinal barrier function-related protein ZO-1 and claudin-1 enhanced when supplemented RA alone, but only claudin-1 was upregulated in the case of RV challenge.

In primary neonatal rat hippocampus, cultures treated with RA (10 nM) demonstrated notable improvements in neuronal survival, a decrease in neuronal ROS levels, and an increase in protein levels of SOD-1 and SOD-2 at 24 and 48 h (Ahlemeyer et al., 2001). Furthermore, the administration of retinoids and RA resulted in a substantial reduction in iron-induced and LPS-induced oxidative stress both in in vitro and in vivo (Lai et al., 2023; Tsuchiya et al., 2009). Consistent with previous findings, we have observed the antioxidative properties of RA in regulating NRF2, a critical transcription factor that activates genes involved in oxidative stress response and detoxification (Ma, 2013; Tonelli et al., 2018), and its downstream target HO-1. On the other hand, our study also investigated the effects of RA supplementation on maintaining redox homeostasis, including GPX4, GSH, MDA, SOD, CAT, and ·OH. Recent findings indicate that the precise regulation of redox signaling by these cells responsible for forming barriers could potentially influence the outcome of an inflammatory event (Gonneaud et al., 2021). Future research should focus on identifying the specific molecular targets of RA and their downstream signaling pathways involved in regulating redox homeostasis against RV challenges.

Autophagy plays a critical role in maintaining cell homeostasis by removing defective proteins and organelles, preventing abnormal protein aggregate accumulation, and removing intracellular pathogens, however, studies about RV infection and its influence on autophagic regulation was limited. Studies showed that RV uses its nonstructural protein 4 to activate a calcium/calmodulin-dependent protein kinase kinase-β and adenosine monophosphate-activated protein kinase (AMPK)-dependent signaling pathway to initiate autophagy, which is hijacked to transport viral proteins to sites of replication and produce infectious virus, but autophagy maturation is blocked (Crawford et al., 2012). In the study carried out by Tian and colleagues (Tian et al., 2016) indicated that RV administration increased the *Beclin* 1 mRNA abundance in porcine jejunum and ileum. These findings demonstrate that RV activates autophagy to enter cells and replicate, but our results show a significant decrease in pBeclin and pULK1 after RV infection, which contradicts previous findings.

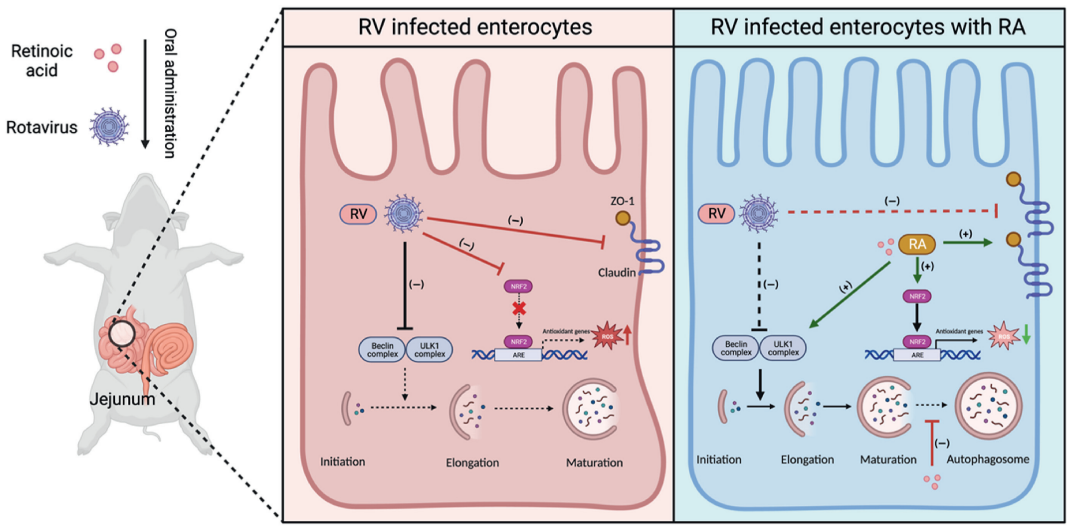

Fig. 6. Diagram illustrating the mechanism by which retinoic acid (RA) mitigates rotavirus (RV)-induced intestinal damage. RV cause intestinal damage and infection possibly through three ways: (1) inhibition of autophagic initiation; (2) impaired NRF2 signaling leading to imbalanced redox hemostasis; (3) intestinal barrier and signaling disruption. RA supplement has the potential to alleviate RV-induced tissue injury and infection partly through following steps: (1) late-stage autophagic flux control; (2) boosting NRF2/HO-1 signaling and protecting redox status; (3) restoring intestinal barrier function and signaling. ZO-1 = zonula occludens-1; Beclin = coiled-coil, moesin-like BCL2-interacting protein; ULK1 = Unc51-like kinase 1; NRF2 = nuclear factor erythroid 2-related factor 2; ROS = reactive oxygen species.

We speculate that RV-induced autophagy may occur in stages, similar to Hantaan virus (HTNV), which triggers complete autophagy at the early stage of infection but incomplete autophagy at the late stage (Wang et al., 2019). RV may activate and inhibit autophagy levels in intestinal cells at different stages of infection to achieve optimal replication. Additionally, we found that adding RA can activate autophagy while inhibiting autophagy flux. To determine which function inhibits RV infection, we used IPEC-J2 intestinal epithelial cells as a model and added RA, E64d, and rapamycin separately. We found that inhibiting autophagy flux effectively inhibits RV virus expression in intestinal epithelial cells. Therefore, we can infer that complete autophagy flux plays a critical role in RV replication.

5. Conclusion

RV cause intestinal damage and infection possibly through three ways: (1) inhibition of autophagic initiation; (2) impaired NRF2 signaling leading to imbalanced redox hemostasis; (3) intestinal barrier and signaling disruption. RA supplement has the potential to alleviate RV-induced tissue injury and infection partly through following steps: (1) late-stage autophagic flux control; (2) boosting NRF2/HO-1 signaling and protecting redox status; (3) restoring intestinal barrier function and signaling, as shown in Fig. 6. In a word, investigating the long-term effects and optimal dosage of RA supplementation on intestinal health could provide valuable information for the development of therapeutic strategies for intestinal diseases.

Author contributions

Xin Lai: Methodology, Software, Formal analysis, Writing – original draft, Project administration. **Aimin Wu:** Formal analysis, Data curation, Conceptualization, Supervision. **Bing Yu:** Visualization, Investigation. **Hui Yan:** Supervision. **Junqiu Luo:** Validation. **Ping Zheng:** Supervision. **Jie Yu:** Data curation. **Daiwen Chen:** Conceptualization, Supervision, Methodology.

Declaration of competing interest

We declare that we have no financial and personal relationships with other people or organizations that can inappropriately influence our work, and there is no professional or other personal interest of any nature or kind in any product, service and/or company that could be construed as influencing the content of this paper.

Acknowledgments

This work was supported by the Joint Funds of the National Natural Science Foundation of China (Grant No. U22A20513). Graphic illustration was designed by Biorender.

References

Ahlemeyer B, Bauerbach E, Plath M, Steuber M, Heers C, Tegtmeier F, et al. Retinoic acid reduces apoptosis and oxidative stress by preservation of SOD protein level. Free Radic Biol Med 2001;30(10):1067–77. https://doi.org/10.1016/s0891-5849(01)00495-6.

Aoyama K, Nakaki T. Glutathione in cellular redox homeostasis: association with the excitatory amino acid carrier 1 (EAAC1). Molecules 2015;20(5):8742–58. https://doi.org/10.3390/molecules20058742.

Szymański Ł, Skopek R, Palusińska M, Schenk T, Stengel S, Lewicki S, et al. Retinoic acid and its derivatives in skin. Cells 2020;9(12):2660. https://doi.org/10.3390/cells9122660.

Baker M, Prasad BVV. Rotavirus cell entry. Curr Top Microbiol Immunol 2010;343:121–48. https://doi.org/10.1007/82_2010_34.

Bose KS, Sarma RH. Delineation of the intimate details of the backbone conformation of pyridine nucleotide coenzymes in aqueous solution. Biochem Biophys Res Commun 1975;66(4):1173–9. https://doi.org/10.1016/0006-291x(75)90482-9.

Buccigrossi V, Laudiero G, Russo C, Miele E, Sofia M, Monini M, et al. Chloride secretion induced by rotavirus is oxidative stress-dependent and inhibited by Saccharomyces boulardii in human enterocytes. PLoS One 2014;9(6):e99830. https://doi.org/10.1371/journal.pone.0099830.

Cao H, Xie J, Guo L, Han K, Pei Y, Li X, et al. All-trans retinoic acid induces autophagic degradation of ubiquitin-like modifier activating enzyme 3 in acute promyelocytic leukemia cells. Leuk Lymphoma 2018;59(5):1222–30. https://doi.org/10.1080/10428194.2017.1365850.

Cheng J, Balbuena E, Miller B, Eroglu A. The role of β-carotene in colonic inflammation and intestinal barrier integrity. Front Nutr 2021;8:723480. https://doi.org/10.3389/fnut.2021.723480.

Crawford SE, Hyser JM, Utama B, Estes MK. Autophagy hijacked through viroporin-activated calcium/calmodulin-dependent kinase kinase-β signaling is required for rotavirus replication. Proc Natl Acad Sci U S A 2012;109(50):E3405–13. https://doi.org/10.1073/pnas.1216539109.

Crawford SE, Criglar JM, Liu Z, Broughman JR, Estes MK. COPII vesicle transport is required for rotavirus NSP4 interaction with the autophagy protein LC3 II and trafficking to viroplasms. J Virol 2019;94(1):e01341–19. https://doi.org/10.1128/JVI.01341-19.

Das K, Roychoudhury A. Reactive oxygen species (ROS) and response of antioxidants as ROS-scavengers during environmental stress in plants. Front Environ Sci 2014;2. https://doi.org/10.3389/fenvs.2014.00053.

Gambhir L, Tyagi G, Bhardwaj R, Kapoor N, Sharma G. Perturbation of cellular redox status: role of Nrf2, a master regulator of cellular redox. In: Ahmad R, editor. Reactive oxygen species. London, UK: IntechOpen; 2022.

Gonneaud A, Turgeon N, Boisvert F-M, Boudreau F, Asselin C. JAK-STAT pathway inhibition partially restores intestinal homeostasis in Hdac1- and Hdac2-intestinal epithelial cell-deficient mice. Cells 2021;10(2):224. https://doi.org/10.3390/cells10020224.

Guerrero CA, Acosta O. Inflammatory and oxidative stress in rotavirus infection. World J Virol 2016;5(2):38–62. https://doi.org/10.5501/wjv.v5.i2.38.

Guo Y, Raev S, Kick MK, Raque M, Saif LJ, Vlasova AN. Rotavirus C replication in porcine intestinal enteroids reveals roles for cellular Cholesterol and sialic acids. Viruses 2022;14(8):1825. https://doi.org/10.3390/v14081825.

He F, Ru X, Wen T. NRF2, a transcription factor for stress response and beyond. Int J Mol Sci 2020;21(13):4777. https://doi.org/10.3390/ijms21134777.

Huang EH, Hynes MJ, Zhang T, Ginestier C, Dontu G, Appelman H, et al. Aldehyde dehydrogenase 1 is a marker for normal and malignant human colonic stem cells (SC) and tracks SC overpopulation during colon tumorigenesis. Cancer Res 2009;69(8):3382–9. https://doi.org/10.1158/0008-5472.CAN-08-4418.

Lai X, Wu A, Bing Y, Liu Y, Luo J, Yan H, et al. Retinoic acid protects against lipopolysaccharide-induced ferroptotic liver injury and iron disorders by regulating Nrf2/HO-1 and RARβ signaling. Free Radic Biol Med 2023;205:202–13. https://doi.org/10.1016/j.freeradbiomed.2023.06.003.

Ma Q. Role of nrf2 in oxidative stress and toxicity. Annu Rev Pharmacol Toxicol 2013;53:401–26. https://doi.org/10.1146/annurev-pharmtox-011112-140320.

Minton K. Intestinal barrier protection. Nat Rev Immunol 2022;22(3):144–5. https://doi.org/10.1038/s41577-022-00685-5.

Molina-Jijón E, Rodríguez-Muñoz R, Del Namorado MC, Bautista-García P, Medina-Campos ON, Pedraza-Chaverri J, et al. All-trans retinoic acid prevents oxidative stress-induced loss of renal tight junction proteins in type-1 diabetic model. J Nutr Biochem 2015;26(5):441–54. https://doi.org/10.1016/j.jnutbio.2014.11.018.

Moroso M, Rozières A, Verlhac P, Komurian-Pradel F, Ferraris O, Peyrefitte CN, et al. The relationship between DUGBE virus infection and autophagy in epithelial cells. Viruses 2022;14(10):2230. https://doi.org/10.3390/v14102230.

Nadarajah KK. ROS homeostasis in abiotic stress tolerance in plants. Int J Mol Sci 2020;21(15):5208. https://doi.org/10.3390/ijms21155208.

Niño DF, Sodhi CP, Egan CE, Zhou Q, Lin J, Lu P, et al. Retinoic acid improves incidence and severity of necrotizing enterocolitis by lymphocyte balance restitution and repopulation of LGR5+ intestinal stem cells. Shock 2017;47(1):22–32. https://doi.org/10.1097/SHK.0000000000000713.

NRC (National Research Council). Nutrient Requirements of Swine. 11th ed. Washington, DC: National Academic Press; 2012.

Patra U, Mukhopadhyay U, Mukherjee A, Sarkar R, Chawla-Sarkar M. Progressive rotavirus infection downregulates redox-sensitive transcription factor Nrf2 and nrf2-driven transcription units. Oxid Med Cell Longev 2020;2020:7289120. https://doi.org/10.1155/2020/7289120.

Pellegrinet L, Rodilla V, Liu Z, Chen S, Koch U, Espinosa L, et al. Dll1- and dll4-mediated notch signaling are required for homeostasis of intestinal stem cells. Gastroenterology 2011;140(4):1230–1240.e1-7. https://doi.org/10.1053/j.gastro.2011.01.005.

Pu J, Chen D, Tian G, He J, Huang Z, Zheng P, et al. All-trans retinoic acid attenuates transmissible gastroenteritis virus-induced inflammation in IPEC-J2 cells via suppressing the RLRs/NF-κB signaling pathway. Front Immunol 2022;13:734171. https://doi.org/10.3389/fimmu.2022.734171.

Qian M, Fang X, Wang X. Autophagy and inflammation. Clin Transl Med 2017;6(1):24. https://doi.org/10.1186/s40169-017-0154-5.

Rajawat Y, Hilioti Z, Bossis I. Autophagy: a target for retinoic acids. Autophagy 2010;6(8):1224–6. https://doi.org/10.4161/auto.6.8.13793.

Rajawat Y, Hilioti Z, Bossis I. Retinoic acid induces autophagosome maturation through redistribution of the cation-independent mannose-6-phosphate

receptor. Antioxid Redox Signal 2011;14(11):2165–77. https://doi.org/10.1089/ars.2010.3491.
Sen A, Namsa ND, Feng N, Greenberg HB. Rotavirus reprograms multiple interferon receptors and restricts their intestinal antiviral and inflammatory functions. J Virol 2020;94(6):e01775–19. https://doi.org/10.1128/JVI.01775-19.
Stanifer M, Boulant S. The origin of diarrhea in rotavirus infection. Science 2020;370(6519):909–10. https://doi.org/10.1126/science.abf1914.
Thomas S, Prabhu R, Balasubramanian KA. Retinoid metabolism in the rat small intestine. Br J Nutr 2005;93(1):59–63. https://doi.org/10.1079/bjn20041306.
Tian G, Liang X, Chen D, Mao X, Yu J, Zheng P, et al. Vitamin D3 supplementation alleviates rotavirus infection in pigs and IPEC-J2 cells via regulating the autophagy signaling pathway. J Steroid Biochem Mol Biol 2016;163:157–63. https://doi.org/10.1016/j.jsbmb.2016.05.004.
Tohmé MJ, Delgui LR. Advances in the development of antiviral compounds for rotavirus infections. mBio 2021;12(3):e00111–21. https://doi.org/10.1128/mBio.00111-21.
Tonelli C, Chio IIC, Tuveson DA. Transcriptional regulation by Nrf2. Antioxid Redox Signal 2018;29(17):1727–45. https://doi.org/10.1089/ars.2017.7342.
Tsuchiya H, Akechi Y, Ikeda R, Nishio R, Sakabe T, Terabayashi K, et al. Suppressive effects of retinoids on iron-induced oxidative stress in the liver. Gastroenterology 2009;136(1):341–350.e8. https://doi.org/10.1053/j.gastro.2008.09.027.
Wang K, Ma H, Liu H, Ye W, Li Z, Cheng L, et al. The glycoprotein and nucleocapsid protein of hantaviruses manipulate autophagy flux to restrain host innate immune responses. Cell Rep 2019;27(7):2075–2091.e5. https://doi.org/10.1016/j.celrep.2019.04.061.
Wang S, Feng R, Shi Y, Chen D, Weng H, Ding H, et al. Intracellular alpha-fetoprotein interferes with all-trans retinoic acid induced ATG7 expression and autophagy in hepatocellular carcinoma cells. Sci Rep 2021;11(1):2146. https://doi.org/10.1038/s41598-021-81678-7.
Wu A, Yu B, Zhang K, Xu Z, de Wu, He J, et al. Transmissible gastroenteritis virus targets Paneth cells to inhibit the self-renewal and differentiation of Lgr5 intestinal stem cells via Notch signaling. Cell Death Dis 2020;11(1):40. https://doi.org/10.1038/s41419-020-2233-6.
Xiang Q, Zhao Y, Lin J, Jiang S, Li W. The Nrf2 antioxidant defense system in intervertebral disc degeneration: molecular insights. Exp Mol Med 2022;54(8):1067–75. https://doi.org/10.1038/s12276-022-00829-6.
Xiao Y, Cai W. Autophagy and viral infection. Adv Exp Med Biol 2020;1207:425–32. https://doi.org/10.1007/978-981-15-4272-5_30.
Yamada S, Kanda Y. Retinoic acid promotes barrier functions in human iPSC-derived intestinal epithelial monolayers. J Pharmacol Sci 2019;140(4):337–44. https://doi.org/10.1016/j.jphs.2019.06.012.
Yin Y, Dang W, Zhou X, Xu L, Wang W, Cao W, et al. PI3K-Akt-mTOR axis sustains rotavirus infection via the 4E-BP1 mediated autophagy pathway and represents an antiviral target. Virulence 2018;9(1):83–98. https://doi.org/10.1080/21505594.2017.1326443.